Journal of Enzyme Inhibition and Medicinal Chemistry

ISSN: 1475-6366 (Print) 1475-6374 (Online) Journal homepage: http://www.tandfonline.com/loi/ienz20

pH-sensitive niosomes: Effects on cytotoxicity and on inflammation and pain in murine models

Federica Rinaldi, Elena Del Favero, Valeria Rondelli, Stefano Pieretti, Alessia Bogni, Jessica Ponti, François Rossi, Luisa Di Marzio, Donatella Paolino, Carlotta Marianecci & Maria Carafa

To cite this article: Federica Rinaldi, Elena Del Favero, Valeria Rondelli, Stefano Pieretti, Alessia Bogni, Jessica Ponti, François Rossi, Luisa Di Marzio, Donatella Paolino, Carlotta Marianecci & Maria Carafa (2017) pH-sensitive niosomes: Effects on cytotoxicity and on inflammation and pain in murine models, Journal of Enzyme Inhibition and Medicinal Chemistry, 32:1, 538-546, DOI: 10.1080/14756366.2016.1268607

To link to this article: http://dx.doi.org/10.1080/14756366.2016.1268607

JOURNAL OF ENZYME INHIBITION AND MEDICINAL CHEMISTRY, 2017
VOL. 32, NO. 1, 538–546
http://dx.doi.org/10.1080/14756366.2016.1268607

Taylor & Francis
Taylor & Francis Group

RESEARCH ARTICLE

OPEN ACCESS

pH-sensitive niosomes: Effects on cytotoxicity and on inflammation and pain in murine models

Federica Rinaldi[a], Elena Del Favero[b], Valeria Rondelli[b], Stefano Pieretti[c], Alessia Bogni[d], Jessica Ponti[d], François Rossi[d], Luisa Di Marzio[e], Donatella Paolino[f,g], Carlotta Marianecci[h] and Maria Carafa[h]

[a]Fondazione Istituto Italiano di Tecnologia, Center for Life Nano Science@Sapienza, Rome, Italy; [b]Department of Medical Biotechnologies and Traslational Medicine, University of Milan, Milan, Italy; [c]Department of Therapeutic Research and Medicine Evaluation, Istituto Superiore di Sanità, Rome, Italy; [d]Consumers and Reference Materials, Consumer Products Safety Unit (F.2), European Commission, Directorate General Joint Research Centre Directorate F – Health, ISPRA, Varese, Italy; [e]Department of Pharmacy, University "G. d'Annunzio", Chieti, Italy; [f]Interregional Research Center for Food Safety & Health (IRC-FSH), Campus Universitario "S. Venuta", University of Catanzaro "Magna Græcia", Catanzaro, Italy; [g]Department of Health Sciences, Campus Universitario "S. Venuta", University of Catanzaro "Magna Græcia", Catanzaro, Italy; [h]Department of Drug Chemistry and Technology, University of Rome "Sapienza", Rome, Italy

ABSTRACT

pH-sensitive nonionic surfactant vesicles (niosomes) by polysorbate-20 (Tween-20) or polysorbate-20 derivatized by glycine (added as pH sensitive agent), were developed to deliver Ibuprofen (IBU) and Lidocaine (LID). For the physical-chemical characterization of vesicles (mean size, size distribution, zeta potential, vesicle morphology, bilayer properties and stability) dynamic light scattering (DLS), small angle X-ray scattering and fluorescence studies were performed. Potential cytotoxicity was evaluated on immortalized human keratinocyte cells (HaCaT) and on immortalized mouse fibroblasts Balb/3T3. *In vivo* antinociceptive activity (formalin test) and anti-inflammatory activity tests (paw edema induced by zymosan) in murine models were performed on drug-loaded niosomes. pH-sensitive niosomes were stable in the presence of 0 and 10% fetal bovine serum, non-cytotoxic and able to modify IBU or LID pharmacological activity *in vivo*. The synthesis of stimuli responsive surfactant, as an alternative to add pH-sensitive molecules to niosomes, could represent a promising delivery strategy for anesthetic and anti-inflammatory drugs.

ARTICLE HISTORY
Received 4 October 2016
Revised 25 November 2016
Accepted 28 November 2016

KEYWORDS
pH-sensitive niosomes; lidocaine; ibuprofen; cytotoxicity; anti-nociceptive/anti-inflammatory activity

Introduction

In several diseases and disorders, acute and chronic inflammation is often associated with pain. Most anti-inflammatory drugs employed for long-term administration for pain relief display extensive adverse effects. Anesthetic and anti-inflammatory preparations show limited efficacy on intact skin and need prolonged applications and high drug concentrations[1–3]. In developing topical formulations, great attention has been devoted to new structures, such as vesicular nanocarriers (e.g. liposomes, niosomes, ethosomes), allowing the localization of the drug within the skin enhancing the local effect or increasing the penetration through the stratum corneum.

Niosomes (NSVs) attracted great attention as nontoxic drug delivery systems in topical/transdermal application for many reasons: NSVs are effective in the modulation of drug release properties; they can act as penetration enhancers through the skin. Their effectiveness is strongly dependent on their physical–chemical properties, such as formulation size, surface charge and lamellarity[4–10].

In this work, niosomes based on polysorbate-20 (Tw20) or its pH-sensitive derivative, polysorbate-20 derivatized by glycine (TW20-GLY), were prepared to investigate the potential application of pH responsive NSV formulation. Ibuprofen and Lidocaine (Supplementary Figure S1) were chosen as model drugs, according to their pharmacological activities on inflammation and pain.

Modification of pH arises in several pathological condition and inflamed tissues often show decreased pH levels and activation of inflammatory mediators when compared with healthy tissues[11]. Nanotherapeutics with increased affinity for an acidic pH microenvironment (i.e. 5.8–7.2) can take advantage of pathological conditions of inflammation for selective targeting[12]. "Fusogenic" vesicles can be also prepared: they are stable at physiological pH (pH 7.4), but undergo destabilization under acidic conditions, leading to the release of their contents at the intracellular level or in inflamed areas[12]. A novel class of compounds based on Tw20 bearing different pH sensitive head groups (i.e. glycine, *N*-methylglycine, *N*,*N*-dimethylglycine) were synthesized by our group to combine niosome delivery features and pH sensitivity as previously demonstrated[13].

In this study, Tween-20 and Tween-20 glycine derivatives were mixed to obtain vesicular carriers loaded with model drugs. Dimensions, ζ-potential, morphology, bilayer features, stability and drug entrapment efficiency (EE) were evaluated in order to better characterize the vesicles. Since the derivatives are primary amines, they could induce toxic effects in healthy cells and tissues. Their potential toxicity was then evaluated on immortalized human keratinocyte cells (HaCaT) and on immortalized mouse fibroblasts

CONTACT Maria Carafa maria.carafa@uniroma1.it Department of Drug Chemistry and Technology, University of Rome "Sapienza", Piazzale A. Moro 5, 00185 Rome, Italy; Carlotta Marianecci carlotta.marianecci@uniroma1.it

Supplemental data for this article can be accessed here.

Balb/3T3 clone A31–1-1, used as *in vitro* models, as alternative to animal tests[14].

Moreover, experiments to assess the *in vivo* efficacy of the drug-loaded niosomes were carried out in murine models to evaluate the potential advantages of stimuli responsive nanocarriers, loaded with Lidocaine or Ibuprofen in pain and inflammation treatments.

Materials and methods

Materials

Tween-20 (Tw20), Sephadex G-75, Hepes salt [*N*-(2-hydroxyethyl) piperazine-*N*-(2-ethanesulfonic acid)], calcein, Ibuprofen and Lidocaine were purchased from Sigma-Aldrich (Sigma-Aldrich SRL, Milan, Italy). Cholesterol (CHOL) and diphenylhexatriene (DPH) were obtained from Acros Organics (Acros Organics BVBA, Geel, Belgium). All other products and reagents were of analytical grade. Tween-20 derivative was synthesized as previously described: briefly, terminal hydroxyl groups were functionalized with glycine (GLY) following the Eschweiler–Clarke reaction[13,15].

Vesicle preparation and purification

Surfactant vesicles (NSVs) were prepared using Tween-20 or Tween-20 glycine derivative and CHOL as reported in Table 1. Where indicated, the fluorescent probe DPH (2×10^{-3} M) or the drugs (Table 1) were added to the surfactant/CHOL mixture before the solubilization in the organic phase. The vesicles were obtained by the "film" method as previously described (see Supplementary data available online)[16–18]. Vesicle dispersions were purified by size exclusion chromatography on Sephadex G-75 glass columns.

Size and ζ-potential measurements of vesicles

Dynamic light scattering (DLS) on a Malvern Zetasizer Nano ZS90 (Malvern Instruments Ltd, Worcestershire, UK) was applied to evaluate the size and the ζ-potential of the NVS dispersions. Reported data represent mean of the ζ-potential (mV) and of the hydrodynamic diameter (nm). NSV samples were diluted 1:100 in HEPES buffer (10 mM, pH7.4) or acetate buffer (200 mM, pH 5.5). The measurement of the breadth of the size distribution (polydispersity index, PDI) value was also evaluated.

Table 1. Sample composition (in bold: selected formulations).

Sample	TW20 (mM)	TW20-GLY (mM)	CHOL (mM)	IBU (%p/v)	LIDO (%p/v)
TW20	15	–	15	–	–
TW20 1% IBU	15	–	15	1	–
TW20 3% IBU	15	–	15	3	–
TW20 5% IBU	15	–	15	5	–
TW20 7% IBU	15	–	15	7	–
TW20 1% LID	15	–	15	–	1
TW20 3% LID	15	–	15	–	3
TW20 5% LID	15	–	15	–	5
TW20 7% LID	15	–	15	–	7
TW20-GLY	3.75	11.25	7.5	–	–
TW20-GLY 1% IBU	3.75	11.25	7.5	1	–
TW20-GLY 3% IBU	3.75	11.25	7.5	3	–
TW20-GLY 5% IBU	3.75	11.25	7.5	5	–
TW20-GLY 7% IBU	3.75	11.25	7.5	7	–
TW2OGLY 1% LID	3.75	11.25	7.5	–	1
TW20-GLY 3% LID	3.75	11.25	7.5	–	3
TW20-GLY 5% LID	3.75	11.25	7.5	–	5
TW20-GLY 7% LID	3.75	11.25	7.5	–	7

Synchrotron small angle X-ray scattering measurements

SAXS measurements were performed at ESRF (Grenoble, France) on ID02 high-brilliance beamline ($\lambda = 0.1$ nm). Samples were put into capillaries (KI-beam; ENKI, Concesio, Italy) and mounted horizontally onto a six-places sample holder, allowing for nearly contemporary measurements on sample and reference cells in the same environmental conditions. All measurements were performed at 25 °C. The exposure time of each measurement was very short, 0.1 s, in order to avoid any radiation damage. The scattered intensity at different angles was collected on a 2D detector and analyzed. The SAXS intensity profiles report the scattered radiation intensity as a function of the momentum transfer q, proportional to the scattering angle, in the region $0.02\,nm^{-1} \leq q \leq 3.5\,nm^{-1}$. To investigate a wide q-region, spectra relative to different q ranges were compared and joined after careful background subtraction. Analysis was carried out to obtain information on size and shape of the particles in solution. The features of the large-scale structure, corresponding to the overall particle, are displayed in the very-low q-region ($q < 0.1\,nm^{-1}$), while the ones of the internal structure can be identified for $q > 0.1\,nm^{-1}$.

Vesicle fluidity determination

DPH was added to vesicle composition at 2×10^{-3} M. DPH-labeled vesicles were prepared as reported above. To avoid any experimental artifact, i.e. to allow the fluorescent probe disposition in the vesicle bilayer, samples were stored 3 h at room temperature before the fluorescence anisotropy experiments. The fluidity of surfactant vesicular membranes was determined by fluorescence anisotropy using DPH as fluorescence probe, as previously reported[18].

Determination of drug EE

Drug entrapment within nonionic surfactant vesicles was determined using high-performance liquid chromatography (HPLC), as previously described, on purified NVS after disruption with isopropanol (vesicle dispersion/isopropanol 1:1 v/v final ratio)[6,19].

Drug EE was calculated as follows:

$$E.E = \frac{Drug_{Ent}}{Drug_{Tot}} \times 100$$

Results are the average of three different batches ± standard deviation.

Vesicle stability evaluation

For colloidal stability at different temperatures, the vesicle formulations were stored at 4 and 25 °C for a period of 90 days. Samples from each batch were withdrawn at definite time intervals (1, 30, 60 and 90 days) and the ζ-potential and the mean of hydrodynamic diameter of vesicles were determined as previously described.

To study the effect of fetal bovine serum (FBS) on vesicle stability calcein-loaded vesicle suspensions (250 μL) were added to 2.25 mL buffer solution in absence (0% FBS) or in presence of 10% of FBS[20,21].

Calcein leakage was evaluated after 3 h and compared to calcein fluorescence intensity (Ex/Em 492/520 nm) after complete leakage by addition of isopropanol (1/1 v/v), detected by means of a Perkin-Elmer LS50B spectrofluorometer (Perkin-Elmer, Waltham, MA). Vesicle size determinations were also performed after incubation. The effect of cell culture medium on vesicle stability was also evaluated on calcein-loaded samples.

Cytotoxicity studies

Cytotoxicity of the vesicles was studied in two different cell lines: immortalized HaCaT cells and immortalized mouse fibroblasts Balb/3T3 clone A31–1-1, using the *in vitro* colony-forming efficiency assay (CFE)[22].

Cell culture conditions

HaCaT cells were originally supplied by the German Cancer Research Center (Heidelberg, Germany) and Balb/3T3 clone A31–1-1 was purchased from Hatano Research Institute (Kanagawa, Japan).

Experimental cultures were prepared from deep-frozen stock vials always maintained in a sub-confluent state (maximum 60–70% confluence) in complete culture medium. HaCaT cells were cultured in DMEM high glucose (Invitrogen, Milan, Italy) supplemented with 10% (v/v) Fetal Clone II serum (Hyclone, Celbio, Italy) and 0.6% (v/v) penicillin/streptomycin (Invitrogen). Balb/3T3 cells were cultured in minimum essential medium (MEM) low glucose supplemented with 10% (v/v) FBS and 0.6% (v/v) penicillin/streptomycin (Invitrogen, Italy). All the cell cultures were maintained in standard cell culture conditions (37 °C, 5% CO_2 and 95% humidity, HERAEUS Incubator, Hanau, Germany).

CFE assay Both cell lines were seeded on 60 × 15 mm Petri dishes (19.3 cm^2 bottom surface area, Corning, Costar, Italy) at a density of 200 cells/dish in 2 mL complete culture medium in three replicates for each treatment condition. After 24 h, the vesicles formulations were directly added to the cell culture to obtain the appropriate final concentrations of 0.1, 0.5, 1, 5, 10, 50 and 100 μg/mL. As a control, the surfactants in non-vesicular formulation were tested at the same concentration range as the vesicular formulation. After 2 or 4 h of exposure for HaCaT and 2 or 24 h of exposure for Balb 3T3, the treatment medium was removed and changed with complete fresh culture medium that was renewed twice a week. After 7 days, cells were fixed for 20 min with 3.7% (v/v) formaldehyde solution (Sigma, Milan, Italy) in phosphate-buffered solution (PBS) (1×, GIBCO, Monza, Italy) and stained for 30 min with 4% (v/v) Giemsa solution (GS-500; Sigma, Milano, Italy) in ultrapure water. Colonies were automatically scored using Gelcount colony counter (Oxford Optronix, Oxford, UK). Each experiment included a negative control (untreated cells in culture medium), a positive control (cells exposed to sodium chromate 100 μM, CAS No. 10034-82-9 Sigma) and a PBS solvent control (cells exposed to the same solvent contained in the stock of niosomes suspension). The results were normalized to the solvent control and expressed as CFE (%) (average number of colonies in treatment/average number of colonies in solvent control, ×100).

In vitro *release*

In vitro release experiments were performed in a flow-through apparatus (EP) at 32 °C in a pH 5.5 buffer. Fixed volumes of vesicle samples were included in dialysis sacs (cut-off 8.000) with a fixed diffusing area (5.5 cm^2). The drug concentration was detected in the outer solution at fixed time intervals by means of the HPLC method described above, taking into account the dilution factor.

In vivo *experiments*

The following experiments were approved by the Service for Biotechnology and Animal Welfare of the Istituto Superiore di Sanità and authorized by the Italian Ministry of Health, according to Legislative Decree 26/2014, which implemented the European Directive 2010/63/UE on laboratory animal protection in Italy. Animal welfare was routinely checked by veterinarians from the Service for Biotechnology and Animal Welfare of the Istituto Superiore di Sanità. TW20 and TW20-GLY loaded with LID or IBU, diluted to obtain the same drug concentration, were compared to: (i) the "unstructured" surfactant formulation and (ii) the "unstructured" surfactant formulation with the same IBU or LID concentration.

Animals, male CD-1 mice (Harlan, Italy) weighing 25–30 g were used for all experiments. Mice were housed for at least 1 week before the experimental sessions in colony cages (seven mice in each cage) under standard light (from 7.00 a.m. to 7.00 p.m.), temperature (21 ± 1 °C), relative humidity (60 ± 10%) with food and water available *ad libitum*.

Formalin test

Subcutaneous injection of a dilute solution of formalin (1%, 20 μL/paw) into the mice hind paw evokes nociceptive behavioral responses, such as licking, biting the injected paw or both, which are considered indices of nociception. The nociceptive response shows a biphasic trend, consisting of an early phase occurring from 0 to 10 min after the formalin injection, due to the direct stimulation of peripheral nociceptors, followed by a late prolonged phase occurring from 15 to 40 min, that reflects the response to inflammatory pain. The total time (s) that the animal spent licking or biting its paw during the formalin-induced early and late phase of nociception was recorded[23]. Samples were administered subcutaneously in the dorsal surface of mice paw 120 min before formalin in a volume of 40 μL/paw.

Zymosan-induced paw edema

Mice received a subcutaneous administration (20 μL/paw) of zymosan (2.5% w:v in saline) into the dorsal surface of the right hind paw[24]. Paw volume was measured three times before the injections and at 1, 2, 3, 4, 24 and 48 h thereafter using a hydroplethysmometer modified for small volumes (Ugo Basile, Varese, Italy). Samples were administered subcutaneously in the dorsal surface of mice paw 120 min before zymosan in a volume of 40 μL/paw. The increase in paw volume was evaluated as percentage difference between the paw volume at each time point and the basal paw volume.

Data analysis and statistics

The statistically significant differences for CFE values versus controls were calculated by the one-way analysis of variance (ANOVA) analysis (GraphPad Prism 4 statistical software, GraphPad Inc., San Diego, CA). Differences were considered statistically significant when $p < 0.05$. Data are presented as average of three independent experiments.

Experimental data from *in vivo* experiments were expressed as mean ± standard error of mean and the significance among the groups was evaluated with the analysis of variance followed by Tukey's post-hoc comparisons using GraphPad Prism 6.03 software. Statistical significance was assumed at least for $p < 0.05$.

Results

Vesicular nanocarrier characterization

The measurements carried out by DLS indicate that vesicular structures with significantly different sizes were obtained, according to

Table 2. Sample characterization.

Sample	Size (nm)	Potential, ζ (mV)	PDI	Fluorescence anisotropy	EE (mg/ml)
TW20	140.8 ± 1.6	−30.4 ± 1.0	0.219 ± 0.04	0.21 ± 0.01	–
TW20 5% IBU	90.6 ± 1.8	−31.7 ± 0.3	0.306 ± 0.09	0.30 ± 0.02	0.28 ± 0.04
TW20 5% LIDO	99.3 ± 1.8	−28.9 ± 0.1	0.133 ± 0.09	0.29 ± 0.01	7.00 ± 0.03
TW20-GLY	215.0 ± 3.0	−41.0 ± 1.2	0.160 ± 0.08	0.17 ± 0.01	–
TW20-GLY IBU 5%	122.1 ± 19.6	−40.2 ± 0.1	0.404 ± 0.05	0.20 ± 0.04	0.18 ± 0.05
TW20-GLY LIDO 5%	121.0 ± 2.3	−42.8 ± 1.3	0.203 ± 0.02	0.23 ± 0.02	8.65 ± 0.04

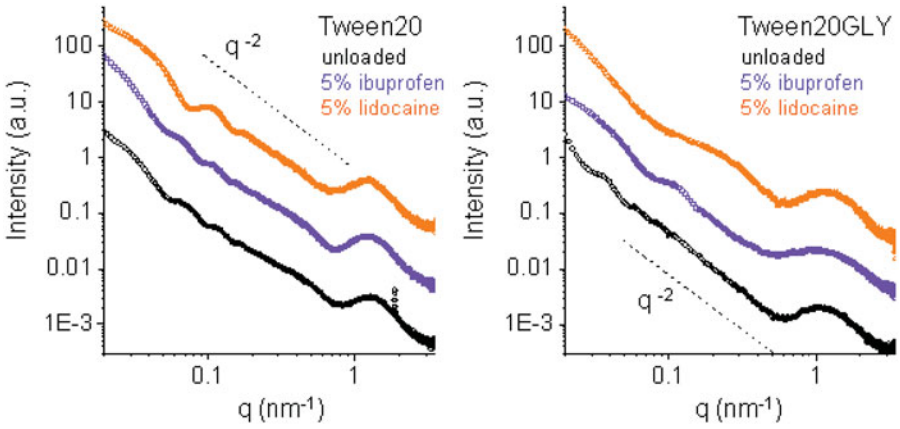

Figure 1. SAXS intensity spectra for Tw20 (left panel) and TW20-GLY (right panel) based systems, at pH 7.4, vertically shifted for enhanced visibility. From bottom to top: unloaded (black), loaded with 5% ibuprofen, loaded with 5% lidocaine. Dash lines decrease with q^{-2} behavior, typical for bilayer structures.

surfactant mixture and drug loaded in NSVs. The interaction of both drugs with Tw20 and TW20-GLY vesicles led to a decrease in vesicle dimensions, when compared to empty ones, without modification of the corresponding ζ-potential values (Table 2).

Furthermore, Tw20- and TW20-GLY-based systems were investigated by Small Angle X-ray scattering to obtain information on the effect of Ibuprofen or Lidocaine loading on the size and shape of the aggregates and on their internal structure.

Figure 1 reports SAXS intensity spectra for Tw20- and TW20-GLY-based systems, at pH 7.4, vertically shifted for enhanced visibility. Spectra display some common features and some peculiarities in all the q range. Analysis of the intensity profiles shows that all Tw20- and TW20-GLY-based systems aggregate in solution as vesicles.

Loaded vesicles are smaller in size (∼100 nm) in both cases, in accordance to what observed by DLS. Actually, the inclusion of drugs in Tw20 and TW20-GLY vesicles led to an increase in fluorescence anisotropy, this related to a decrease in bilayer fluidity (Table 2). Furthermore, a higher E.E. was observed in Lidocaine-loaded samples when compared to Ibuprofen-loaded ones (Table 2)

Lidocaine, embedded in the bilayer, gives a higher spontaneous curvature to the aggregate. In the Tween20-based system (see orange points, left panel, Figure 1), this behavior results in quite monodisperse round shaped vesicles. The characteristic SAXS intensity profile has been reproduced, as reported in Supplementary Figure S2, with the form factor of a spherical hollow particle (external radius 46 nm) with a shell constituted by a bilayer with thickness of 6 nm. In the TW20-GLY system, the SAXS intensity profile of loaded niosomes (orange points, right panel, Figure 1) displays a different behavior, with both a shift and a partial filling of the first intensity minimum. On the local scale, all vesicles are constituted by a single bilayer, as visible in Figure 1 from the typical q^{-2} behavior of the intensity profile. The transverse structure of the bilayers affects the high q-region of the intensity spectra. In the case of TW20-GLY vesicles, the high q-region of the intensity profile ($q > 0.4\,nm^{-1}$) is altered by the presence of Ibuprofen.

Unloaded vesicles are stable for at least 6 months when stored at 4 °C and at least 3 months when stored at 25 °C (data not shown). Drug-loaded samples, in spite of the decrease in bilayer fluidity, are stable only for 1 month when stored at 25 °C (data not shown). Difference in bilayer fluidity does not affect vesicle stability, whereas drug release is affected by this parameter (Figure 2(A,B)): TW20-GLY samples (Figure 2(B)), with high bilayer fluidity, show higher drug release compared to Tween-20 samples (Figure 2(A)).

To better simulate *in vivo* conditions, all tested samples were analyzed at pH 7.4 in the presence of 0 and 10% FBS. The addition of serum to surfactant vesicular formulations at pH 7.4 did not modify significantly the vesicle stability (i.e. the percentage of calcein released after 3 h, for further details see Supplementary Figure S3).

CFE

Changes in cell viability of Balb/3T3 and HaCaT cells, after exposure to Tw20 and TW20-GLY formulations at concentrations ranging from 0.10 to 100 μM, were evaluated by the CFE assay. The Balb/3T3 cells were treated with Tw20 and TW20-GLY formulations, Tween-20 control and Tween-20 glycine control (material not in vesicular form) for 2 and 24 h and HaCaT cells for 2 and 4 h. Results are expressed as percentage of CFE versus the solvent control and they are average of three independent experiments, with three replicates for each experimental point (Figures 3 and 4). The solvent control (PBS at the same concentration used for analyzed formulation) did not induce any cytotoxicity compared to the negative control. Treatment with the positive control resulted in complete cell death, as expected (data not shown).

Balb/3T3 cells incubated with Tw20 formulation and with Tween-20 control for 2 h (Figure 3(A)) show no statistically

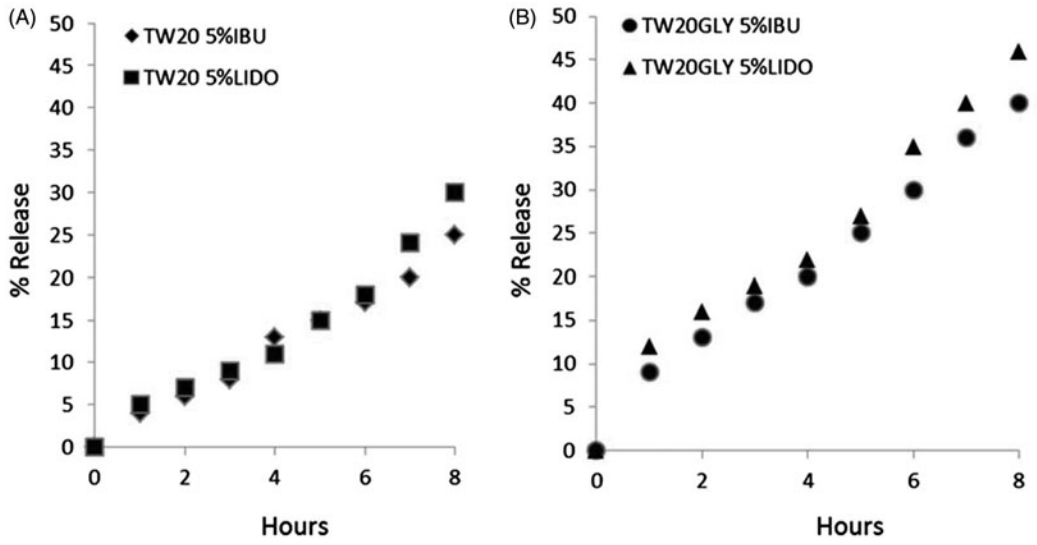

Figure 2. Release profiles of IBU and LID from the vesicular carriers in HEPES (pH =7.4) at 32 °C as a function of time: (A) TW20 samples; (B) TW2–0GLY samples. Release experiments were carried out in triplicate. The reported value represents mean values and lay within 10% of the mean.

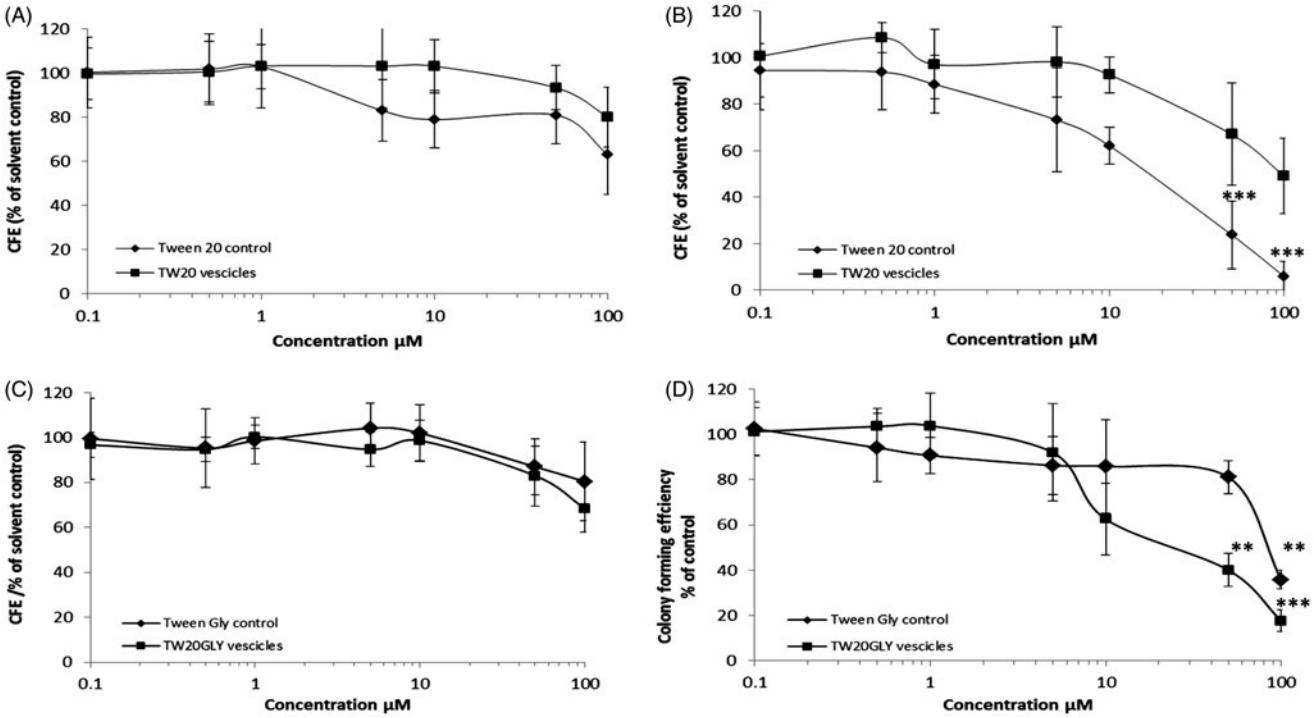

Figure 3. Cytotoxic effects of TW20 and TW20-GLY on Balb-3T3 cells as evaluated by CFE assay. Cells were exposed to increasing concentrations (0.1–100 µM) of Tw20 formulation and to the same concentration of Tween 20 control for 2 h (A) and 24 h (B) and to increasing concentrations (0.1–100 µM) of TW20GLY formulation and of Tween-20 glycine control not in vesicular form for 2 h (C) and for 24 h (d). In this range of concentrations, statistically significant cytotoxicity was found in Balb/3T3 cells exposed for 24 h to Tween-20 control at 50 µM and 100 µM (***$p < 0.0001$) but not to the Tw20 vesicles at the same concentrations. Statistically significant cytotoxicity was also found in cells exposed to Tw20GLY formulation at 50 µM (**$p < 0.001$) and 100 µM (***$p < 0.0001$) but not to the Tween-20 glycine control at the same concentrations.

significant cytotoxicity at all concentrations tested. After 24 h of incubation (Figure 3(B)), statistically significant cytotoxicity was found in Balb/3T3 cells exposed to Tween-20 control at 50 and 100 µM (***$p < 0.0001$) but not to the Tw20 formulations at the same concentrations. The calculated IC_{50} for Tween-20 control and Tw20 formulations after 24 h of incubation, are respectively of 64.8 ± 5.5 and 25.3 ± 13.2 µM (Hill's Function, Graph Pad Prism). IC_{50} for Tw20 and for Tween-20 control after 4 h of incubation is higher than 100 µM (maximum concentration tested).

Balb/3T3 cells incubated with TW20-GLY formulation and with Tween 20 glycine control for 2 h (Figure 3(C)) show no statistically significant cytotoxicity at all tested concentrations. After 24 h of incubation (Figure 3(D)), statistically significant cytotoxicity was found in Balb/3T3 cells exposed to TW20-GLY formulation at 50 µM (**$p < 0.001$) and 100 µM (***$p < 0.0001$) and to Tween-20 glycine control at 100 µM (**$p < 0.001$). At 24 h incubation, the IC_{50} of TW20-GLY formulations is of 25.8 ± 8.3 µM and the IC_{50} of Tween-20 glycine control is of 61.7 ± 2 µg/mL. IC_{50} for TW20-GLY

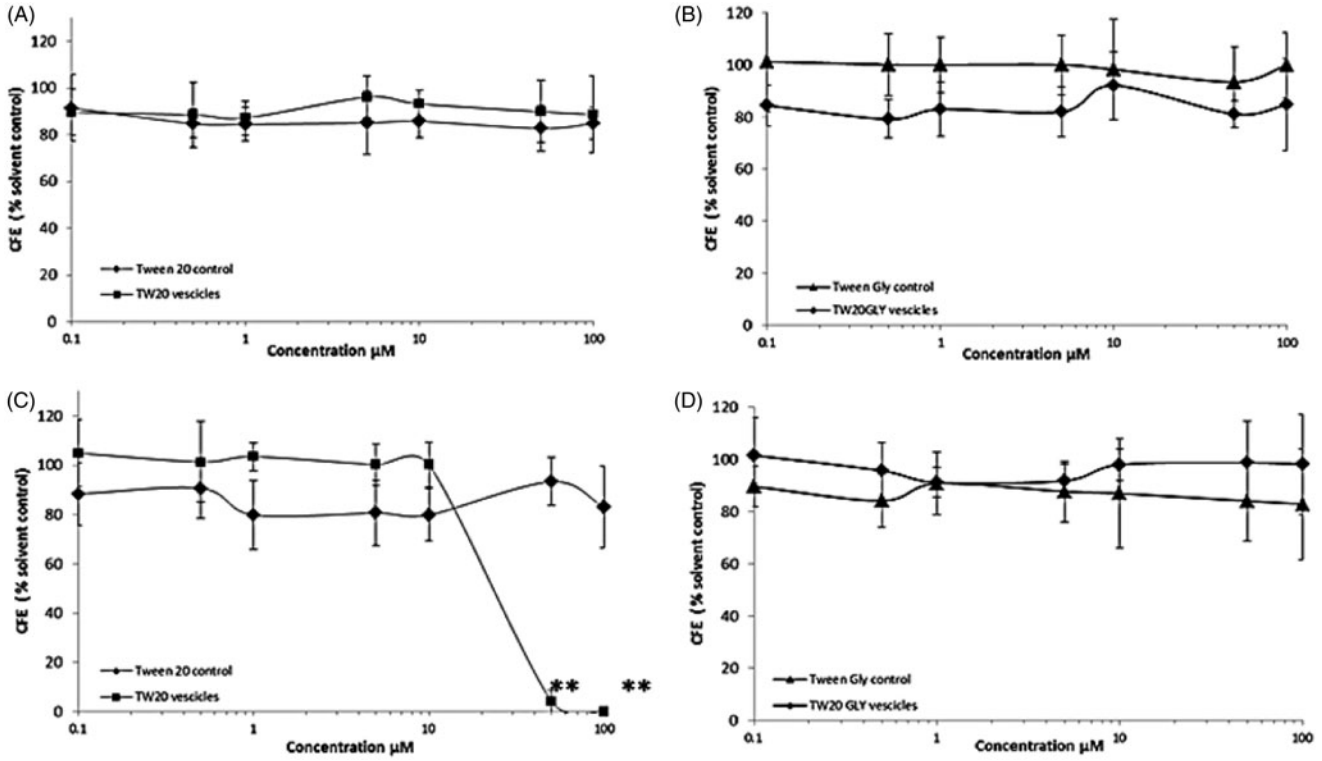

Figure 4. Cytotoxic effects of TW20 and TW-20GLY on HaCaT cells evaluated by CFE assay. HaCaT cells were exposed to increasing concentration of TW20 formulation and to the same concentration of Tween-20 control for 2 h (A) and 4 h (B) and to increasing concentrations (0.1–100 μM) of TW20-GLY formulation and of Tween-20 glycine control for 2 h (C) and for 24 h (d). In this range of concentrations, statistically significant cytotoxicity was observed only in HaCat cells exposed to TW20 formulation at 50 and 100 μM (**$p < 0.001$).

and Tween-20 glycine control after 4 h of incubation, is higher than 100 μM. Both Tw20 and TW20-GLY formulations started to show a dose effect relationship at 24 h of incubation.

HaCaT cells exposed for 2 h to Tw20 formulation and Tween-20 control (Figure 4(A)) and to TW20-GLY formulation and Tween-20 glycine control (Figure 4(B)) show no cytotoxicity at all tested concentrations. After 4 h of incubation with TW20-GLY vesicles and Tween-20 glycine control (Figure 4(C)) no cytotoxicity was observed (IC_{50} is higher than the tested concentration). The 4 h exposure to Tw20 formulation shows a statistically significant cytotoxic effect at 50 and 100 μM (**$p < 0.001$), while no cytotoxicity was observed for the Tween-20 control at the same concentrations. The calculated IC_{50} for Tw20 formulation is 32.9 ± 9.2 μM, for the Tween-20 control is higher than 100 μM and 100 μg/mL, respectively.

In vivo *experiments*

The results obtained in the formalin test are reported in Figure 5(A,B). The administration of the surfactant solution (V) did not change the response to formalin both in the early and in the late phase of the test. When IBU or LID were administered together with TW20 empty vesicles or loaded in TW20 vesicles in the mice paw before formalin we did not observe any differences in the paw licking induced by formaldehyde. On the contrary, pH-sensitive vesicles loaded with IBU or LID were able to strongly reduce licking activity induced by formalin in both test phases. The effects of IBU loaded vesicles on edema development induced by zymosan are reported in Figure 6. The administration of vesicles alone, IBU and TW20 vesicles or IBU in TW20 vesicles did not change paw edema increase. When IBU loaded pH-sensitive vesicles were administered before zymosan, a significant reduction in paw volume development was recorded. The reduction in paw volume increase started 1 h after zymosan administration and was still present 24 h thereafter.

Discussion

The surfactant vesicles, prepared with the mixture of surfactants, CHOL and drugs at different molar ratio (Table 1), showed size and ζ-potential values not always useful for proposed *in vivo* application (data not shown); for this reason only the results on samples with higher EE (Table 2) are reported and discussed.

Tw20 and TW20-GLY based systems were investigated by small angle X-ray scattering to obtain information on the effect of Ibuprofen or Lidocaine on vesicle features. SAXS data are in good agreement with DLS results: vesicle sizes are quite different for the different systems, being larger for the TW20-GLY unloaded vesicles (215 nm) with respect to the Tw20 ones (140 nm). Taking into consideration the derivatization of PEG chains, it can be assumed that the reported data may be connected to differences in the solvation state of PEG polymeric chains[25].

Loaded vesicles, maintaining the single bilayer structure, are smaller in size (∼100 nm) in both cases, in accordance to what observed by DLS; this is reasonably related to an higher spontaneous curvature due to the partial inclusion of amphiphilic drugs in vesicle bilayer, leading to a decrease in their bilayer fluidity.

The slighter decrease in vesicle bilayer fluidity of TW20-GLY samples (Table 2) could be related to a partial "partition" of the drug between hydrophobic and hydrophilic regions. SAXS results on the local structure of TW20-GLY bilayer could confirm that the presence of Ibuprofen within the bilayer affects not only the hydrophobic core, but also its hydrophilic regions.

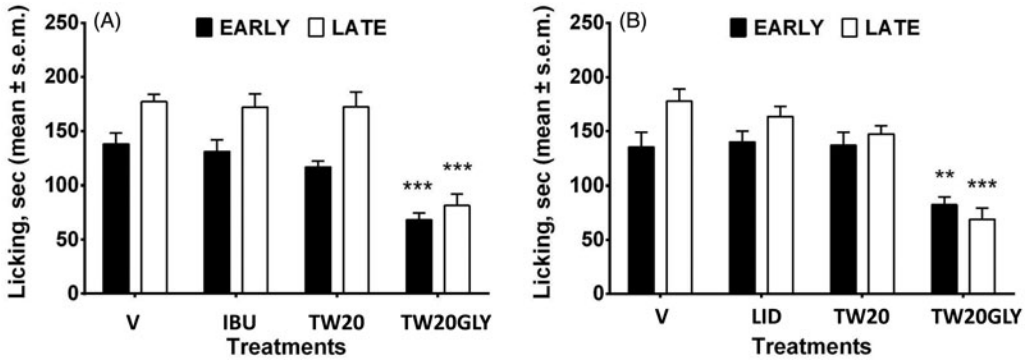

Figure 5. *In vivo* effects of drug-loaded nonionic surfactant vesicles on formalin-induced nociception (IBU: panel A; LID: panel B). Purified formulation of vesicles and drug solution at the same drug concentration were used. The data are considered to be statistically significant for *Pb0.05, **Pb0.01 and ***Pb0.001 versus vehicle-treated animals (HEPES buffer). $N = 9–10$.

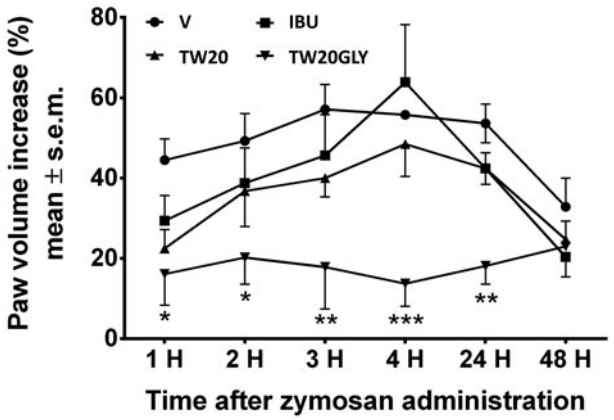

Figure 6. *In vivo* effects of drug-loaded vesicles in edema induced by zymosan. Purified formulation of vesicle and drug solution at the same drug concentration were used. The data are considered to be statistically significant for *Pb0.05, **Pb0.01 and ***Pb0.001 versus vehicle-treated animals (HEPES buffer). $N = 10–12$.

Lidocaine higher EE in Tw20 and TW20-GLY samples is in agreement with the Lidocaine molecule interaction with the hydrophobic moiety of Tweens previously reported[26,27]. Reduced Ibuprofen drug loading could be related to electrostatic repulsive forces between the carboxyl group of Ibuprofen and the polar niosome surface (Table 2)[28].

Actually, Lidocaine, entrapped in both vesicular structures in higher amount than Ibuprofen, seems to display a larger effect on vesicles size and shape: SAXS results indicate a change of the niosomes form factor from spherical vesicles to elongated, ellipsoidal vesicles, induced by the presence of Lidocaine within the closed bilayer. The potential *in vivo* use of vesicle formulations is also related to their stability at different storage temperature and in the presence of 0 and 10% FBS[29].

Decreased drug-loaded vesicle stability when stored at 25 °C (1 month) could be affected by the decrease of vesicle size leading to an increase of the interfacial curvature free energy[30]. On the other hand, the addition of serum at pH 7.4 did not modify significantly the vesicle stability (Figure 4).

Since TW20-GLY is a primary amine, potentially toxic in healthy cells and tissues, cytotoxicity was evaluated on HaCaT and Balb/3T3 clone A31–1-1 cells. The obtained results show that the niosomes are not toxic to the cells: they only show toxicity at high concentration and for prolonged exposure (Figures 5 and 6).

In order to choose the better formulation to be tested in *in vivo* experiments, release studies were carried out. TW20-GLY samples (Figure 3(B)), with high bilayer fluidity, show higher drug release compared to Tween-20 samples (Figure 3(A)), this being probably related to drug diffusion through vesicle bilayer rather than to vesicle disruption. The lipid composition of vesicles can influence the entrapment and the release of sparingly soluble drugs with a general correlation between release rates and bilayer fluidity of vesicle bilayer with decreased release rate with limited bilayer fluidity[28,31]. The presence of cholesterol induces membrane stability via an interaction between the rigid hydrophobic ring structure of the molecule and the alkyl side-chains of amphiphilic molecules, which ultimately decreases membrane fluidity[32]. It can be assumed that cholesterol hinders the drug incorporation within the bilayer because of its bulky nature. This effect is less evident in TW20-GLY samples, incorporating a lower amount of cholesterol as compared to TW20 samples (Table 1). Self-assembly is at the basis of niosomes formation. The final structure of the niosome results from the interplay among all the different molecules packing requirements, their lateral distribution within each layer (internal and external) and their asymmetric disposition within the two layers.

In both systems, the presence of drug induces a marked reduction in size of the vesicles, corresponding to an increase in the spontaneous curvature. Loaded bilayers can close in smaller, highly curved particles, thanks to the presence within the bilayer of an additional component, the drug, that can be distributed non-uniformly both laterally and transversely inside the hydrophobic core. Moreover, in TW20 and TW20-GLY, self-assembled niosomes cholesterol can be partially excluded from the bilayer or can be present in the form of crystallites[33,34]. The presence of an additional amphiphilic component may change the amount and the distribution of cholesterol within the two leaflets of the bilayers.

The best behavior in "*in vitro*" release experiments of pH-sensitive vesicles (samples TW20-GLY 5% LIDO and TW20-GLY 5% IBU, Table 1) was confirmed in "*in vivo*" experiments in murine models highlighting the potential advantages of *stimuli* responsive nanocarriers in pain and inflammation treatments. Niosomes containing pH-sensitive components, such as TW20-GLY that protonate at lower pH, show a destabilization of the carrier bilayer, probably due to the segregation or leakage of cholesterol[33].

The increased fluidity of the bilayer allows a higher *in vitro* drug release if compared to Tween-20 samples (Figure 3) and an enhanced therapeutic effects in *in vivo* pain and inflammation models.

Conclusion

Many different interactions are present in complex structures, such as pharmaceutical formulations. The "deconstruction" of the

carriers may be a crucial step to engineer novel ways to deliver drugs and represents the crossroad of an interdisciplinary effort to develop strategies to combat different diseases.

An essential tool in the pharmaceutical application of vesicular carriers as delivery systems for drugs is their efficient and stable encapsulation of such drugs. In the present work, we have shown that niosomes could be prepared to entrap drugs with different stability and release characteristics, with the drug entrapment capacity being dependent on the surfactant used and the physical-chemical characteristics of the drug.

The TW20 and TW20-GLY niosomes formulations are stable and nontoxic and were tailored for the optimization of their pharmaceutical properties, such as drug release rate and *in vivo* anti-nociceptive and anti-inflammatory activity. *In vivo* tests of TW20-GLY loaded with IBU and LID show the efficiency of the drug delivery as compared to the free active principle, therefore confirming the interest of the pH-sensitive nanocarrier formulation.

Thus, the synthesis of novel stimuli responsive surfactant, as an alternative to add pH-sensitive molecules to niosome formulation, represents an effective and promising delivery strategy, which may greatly increase the utility of niosomes as a targeted delivery vehicle which is degraded only in the target area, where the drug will be released and accumulated. On the other hand, the carrier can be evenly distributed within the circulation since at physiological pH the TW20-GLY niosomes have chemical–physical properties, that will promote their half time of circulation and hence biodistribution by avoiding their capture by reticuloendothelial system, due to the presence of PEG chains on the polar head group of TW20.

Acknowledgements

We thank T. Narayanan and ID02 beamline staff (ESRF) for technical support. This work was supported by Italian Institute of Technology (IIT) Center for Life Nano Science@Sapienza and the NanoMED project of the JRC Institutional program.

Disclosure statement

The authors report no conflicts of interest. The authors alone are responsible for the content and writing of this article.

References

1. Dalili H, Adrian J. The efficacy of local anesthetics in blocking the sensations of itch, burning, and pain in normal and "sunburned skin". Clin Pharmacol Ther 1971;12:913–19.
2. Muzzalupo R, Tavano L. Niosomal drug delivery for transdermal targeting: recent advances. Res Rep Transderm Drug Deliv 2015;4:23–33.
3. Giese U. Absorption and distribution of ibuprofen from a cream formulation after dermal administration to guinea pigs. Arzneimittelforschung 1990;40:84–8.
4. Marianecci C, Di Marzio L, Rinaldi F, et al. Niosomes from 80s to present: the state of the art. Adv Colloid Interface Sci 2014;205:187–206.
5. Maibach HI, Choi MJ. Liposomes and niosomes as topical drug delivery systems. Skin Pharmacol Physiol 2005;18:209–19.
6. Carafa M, Marianecci C, Rinaldi F, et al. Span and Tween neutral and pH-sensitive vesicles: characterization and *in vitro* skin permeation. J Liposome Res 2009;19:332–4.
7. Marianecci C, Carafa M, Di Marzio M, et al. A new vesicle-loaded hydrogel system suitable for topical applications: preparation and characterization. J Pharm Pharmaceut Sci 2001;14:336–46.
8. Di Marzio L, Marianecci C, Rinaldi F, et al. Deformable surfactant vesicles loading ammonium glycyrrhizinate: characterization and *in vitro* permeation studies. Lett Drug Des Discov 2012;9:494–9.
9. Marianecci C, Rinaldi F, Mastriota M, et al. Anti-inflammatory activity of novel ammonium glycyrrhizinate/niosomes delivery system: human and murine models. J Control Rel 2012;164:17–25.
10. Marianecci C, Rinaldi F, Di Marzio L, et al. Ammonium glycyrrhizinate-loaded niosomes as potential nanotherapeutic system for anti-inflammatory activity in murine models. Int J Nanomed 2014;9:635–51.
11. Wiig H. Pathophysiology of tissue fluid accumulation in inflammation. J Physiol 2011;589:2945–53.
12. Lehner R, Wang X, Wolf M, Hunziker P. Designing switchable nanosystems for medical application. J Control Release 2012;161:307–16.
13. Masotti A, Vicennati A, Alisi A, et al. Novel Tween-20 derivatives enable the formation of efficient pH-sensitive drug delivery vehicles for human hepatoblastoma. Bioorg Med Chem Lett 2010;20:3021–5.
14. Broggi F, Mariani V, et al. Morphological transformation induced by multiwall carbon nanotubes on Balb/3T3 cell model as an in vitro end point of carcinogenic potential. Nanotoxicology 2013;7:221–33.
15. Clarke HT, Gillespie HB, Weisshauss SZ. The action of formaldehyde on amines and amino acids. J Am Chem Soc 1933;55:4571–87.
16. Di Marzio L, Marianecci C, Petrone M, et al. Novel pH-sensitive non-ionic surfactant vesicles: comparison between Tween 21 and Tween 20. Colloids Surf B Biointerfaces 2011;82:18–24.
17. Marianecci C, Rinaldi F, Di Marzio L. Interaction of pH-sensitive non-phospholipid liposomes with cellular mimetic membranes. Biomed Microdevices 2013;15:299–309.
18. Carafa M, Marianecci C, Lucania G, et al. New vesicular ampicillin-loaded delivery systems for topical application: characterization, *in vitro* permeation experiments and antimicrobial activity. J Control Release 2004;95:67–74.
19. Marianecci C, Rinaldi F, Di Marzio L, et al. Polysorbate 20 vesicles as multi-drug carriers: *in vitro* preliminary evaluations. Lett Drug Design Discov 2013;10:212–18.
20. Carafa M, Di Marzio L, Marianecci C, et al. Designing novel pH-sensitive non-phospholipid vesicle: characterization and cell interaction. Eur J Pharm Sci 2006;28:385–93.
21. Hossann H, Wiggenhorn M, Schwerdt A, et al. *In vitro* stability and content release properties of phosphatidylglyceroglycerol containing thermosensitive liposomes. Biochim Biophys Acta 2007;1768:2491–9.
22. Ponti J, Colognato R, Rauscher H, et al. Colony forming efficiency and microscopy analysis of multi-wall carbon nanotubes cell interaction. Toxicol Lett 2010;197:29–37.
23. Pieretti S, Di Giannuario A, De Felice M, et al. Stimulus-dependent specificity for annexin 1 inhibition of the inflammatory nociceptive response: the involvement of the receptor for formylated peptides. Pain 2004;109:52–63.
24. Pieretti S, Dominici L, Di Giannuario A, et al. Local anti-inflammatory effect and behavioral studies on new PDE4 inhibitors. Life Sci 2006;79:791–800.

25. Pippa N, Psarommati F, Pispas S, Demetzos C. The shape/morphology balance: a study of stealth liposomes via fractal analysis and drug encapsulation. Pharm Res 2013;30:2385–95.
26. Goddart ED, Anathapadmanabhan G, Interaction of surfactants with polymers and proteins. Boca Raton, FL: CRC Press; 1993:345–8.
27. Carafa M, Santucci E, Lucania G. Lidocaine-loaded non-ionic surfactant vesicles: characterization and *in vitro* permeation studies. Int J Pharm 2002;231:21–32.
28. Mohammed A, Weston N, Coombes AGA, et al. Liposome formulation of poorly water soluble drugs: optimisation of drug loading and ESEM analysis of stability. Int J Pharm 2004;285:23–34.
29. Fattal E, Couvreur P, Dubernet C. "onic pH-sensitive liposomes" delivery of antisense oligonucleotides by anionic pH-sensitive. Adv Drug Deliv Rev 2004;56:931–46.
30. dos Santos S, Medronho B, dos Santos T, Antunes FE. Amphiphilic molecules in drug delivery systems. In: Jorge C, ed. Drug delivery systems: advanced technologies potentially applicable in personalised treatment. Amsterdam, the Netherlands: Springer; 2013:35–85.
31. Ali MH, Kirby DJ, Mohammed AR, Perrie Y. Solubilisation of drugs within liposomal bilayers: alternatives to cholesterol as a membrane stabilising agent. J Pharm Pharmacol 2010;62:1646–55.
32. Kirby C, Gregoriadis G. Effect of the cholesterol content of small unilamellar liposomes on their stability *in vivo* and *in vitro*. Biochem J 1980;186:591–8.
33. Marianecci C, Di Marzio L, Del Favero E, et al. Niosomes as drug nanovectors: multiscale pH-dependent structural response. Langmuir 2016;32:1241–9.
34. Pozzi D, Caminiti R, Marianecci C, et al. Effect of cholesterol on the formation and hydration behaviour of solid-supported niosomal membranes. Langmuir 2010;26:2268–73.